

Phase modulation of directed transport, energy diffusion and quantum scrambling in a Floquet non-Hermitian system

Wen-Lei Zhao,^{1,*} Guanling Li,¹ and Jie Liu^{2,3,†}

¹*School of Science, Jiangxi University of Science and Technology, Ganzhou 341000, China*

²*Graduate School of China Academy of Engineering Physics, Beijing 100193, China*

³*CAPT, HEDPS, and IFSA Collaborative Innovation Center of the Ministry of Education, Peking University, Beijing 100871, China*

(Dated: December 14, 2023)

We investigate both theoretically and numerically the wavepacket's dynamics in momentum space for a Floquet non-Hermitian system with a periodically-kicked driven potential. We have deduced the exact expression of a time-evolving wavepacket under the condition of quantum resonance. With this analytical expression, we can investigate thoroughly the temporal behaviors of the directed transport, energy diffusion and quantum scrambling. We find interestingly that, by tuning the relative phase between the real part and imaginary part of the kicking potential, one can manipulate the directed propagation, energy diffusion and quantum scrambling efficiently: when the phase equals to $\pi/2$, we observe a maximum directed current and energy diffusion, while a minimum scrambling phenomenon protected by the \mathcal{PT} -symmetry; when the phase is π , both the directed transport and the energy diffusion are suppressed, in contrast, the quantum scrambling is enhanced by the non-Hermiticity. Possible applications of our findings are discussed.

I. INTRODUCTION

Engineering the wavepacket's dynamics, such as directed transport [1–4], energy diffusion [5–9] and information scrambling [10–12], is of great interest both theoretically and experimentally across various fields of physics [13, 14]. The phase incorporated in Floquet driven potentials is vitally a knob to manipulate the quantum dynamics [15]. For example, the temporal modulation of the phase of laser standing waves can be used to create artificial gauge fields for ultracold neutral atoms, mimicking the transport behavior of electrons in a synthetic nanotube, with the Aharonov-Bohm flux controllable by the phase [16–18]. The quasiperiodically modulated phase of the external driven potential even induces the formation of synthetic dimension [19–22], wherein the Anderson metal-insulator transition of disorder systems is experimentally observed by using a variant of the kicked rotor model [23–25]. More significantly, complex potentials are achievable in atom-optical experiments, where precise control over the relative phase between the real and imaginary components of this non-Hermitian potential allows for the realization of distinct symmetry classes of systems [26, 27].

Nowadays, non-Hermiticity is widely acknowledged as a fundamental extension of conventional quantum mechanics [28, 29] due to its natural incorporation of the gain and loss or non-reciprocity in diverse systems like photonic crystals [30–35], acoustic arrays [36, 37], and electrical circuits [38, 39]. The emergence of the complex eigenspectra of non-Hermitian systems gives rise to rich phenomena with no Hermitian counterpart. For exam-

ple, as the system adiabatically crosses the exceptional points at which both the eigenvalues and eigenstates coalesce, the Landau-Zener tunneling emerges, indicating the breakdown of adiabaticity [40–43]. The spontaneous \mathcal{PT} -symmetry breaking induces the quantized acceleration of directed transport [44] and the quantized response of quantum scrambling [45] in non-Hermitian chaotic systems [46]. In addition, various topological symmetry classes, including point gap and line gap eigenbands in the complex plane, have been recognized as having significant impacts on edge-state transport behavior, for instance non-Hermitian skin effects [47–49]. Besides, the non-Hermitian potential can be engineered effectively in versatile platforms of photonic systems [50, 51] and atom-optics [27], which unveils the possibilities for manipulating the wavepacket's dynamics in a controllable manner.

In this context, we investigate both theoretically and numerically the phase modulation of the directed transport, energy diffusion, and quantum scrambling, in a non-Hermitian quantum kicked rotor (NQKR) model with quantum resonance condition. We find that the relative phase between the real part and imaginary part of the kicking potential dominates the wavepacket's dynamics. Specifically, as time evolves, the direct current undergoes a transition from quadratic growth, dependent on the non-Hermitian driving strength, to linear growth, which becomes independent of the non-Hermitian driving strength. Such a dynamical crossover from non-Hermiticity dependent regime to non-Hermiticity independent regime is also observed in the ballistic diffusion of mean energy. Furthermore, we unveil the quadratic growth in the OTOCs during the initial stages of time evolution and a transition to linear growth after a sufficiently long period, both influenced by the non-Hermitian driving strength. Interestingly, when the phase equals to $\pi/2$ ensuring \mathcal{PT} -symmetry, we observe a maximum transport behavior and a minimum scram-

*wzhao@jxust.edu.cn

†jliu@gscaep.ac.cn

bling phenomenon. At a phase of π , both the directed transport and the energy diffusion are suppressed, in contrast the quantum scrambling is enhanced by the non-Hermiticity. Our findings provide theoretical guidance for Floquet engineering of quantum dynamics in non-Hermitian systems, which has significant implications in various physics fields, including quantum chaotic control and condensed matter physics.

The paper is organized as follows. In Sec. II we describe the system and show the phase modulation of wavepacket's dynamics with emphasising on the directed current, energy diffusion and quantum scrambling. A summary is presented in Sec. III.

II. NQKR MODEL AND MAIN RESULTS

The dimensionless Hamiltonian of the NQKR reads

$$\mathcal{H} = \frac{p^2}{2} + V_K(\theta) \sum_n \delta(t - t_n), \quad (1)$$

with the kicking potential

$$V_K(\theta) = K \cos(\theta) + i\lambda \cos(\theta + \phi), \quad (2)$$

where $p = -i\hbar_{\text{eff}}\partial/\partial\theta$ is the angular momentum operator, θ is the angle coordinate, satisfying the commutation relation $[\theta, p] = i\hbar_{\text{eff}}$ with \hbar_{eff} the effective Planck constant. The parameters K and λ represent the strength of the real and imaginary components of the kicking potential, respectively. The relative phase between these two components is determined by the parameter ϕ . This kind of complex potential has been realized in the atom-optics experiment [27]. The eigenequation of angular momentum operator is $p|\varphi_n\rangle = p_n|\varphi_n\rangle$ with eigenvalue $p_n = n\hbar_{\text{eff}}$ and eigenstate $\langle\theta|\varphi_n\rangle = e^{in\theta}/\sqrt{2\pi}$. With the completed basis of $|\varphi_n\rangle$, an arbitrary state can be expanded as $|\psi\rangle = \sum_n \psi_n|\varphi_n\rangle$. One-period evolution of the quantum state from t_n to t_{n+1} is governed by $|\psi(t_{n+1})\rangle = U|\psi(t_n)\rangle$, where the Floquet operator $U = U_f U_K$ is composed of the free evolution $U_f = \exp(-ip^2/2\hbar_{\text{eff}})$ and the kicking evolution $U_K = \exp[-iV_K(\theta)/\hbar_{\text{eff}}]$.

In the main quantum resonance situation $\hbar_{\text{eff}} = 4\pi$, each matrix elements of U_f is unity, i.e., $U_f(p_n) = \exp(-in^2 2\pi) = 1$, therefore, it has no effects on the time evolution of quantum states. One can get the exact express of the quantum state after arbitrary kick period, i.e., $|\psi(t)\rangle = U_K^t|\psi(t_0)\rangle$. Without loss of generality, we choose the ground state of the angular momentum operator as the initial state, i.e., $\psi(\theta, t_0) = 1/\sqrt{2\pi}$. Then, the quantum state $|\psi(t)\rangle$ in coordinate space has the expression

$$\psi(\theta, t) = \frac{1}{\sqrt{2\pi}} \exp\left\{\frac{-it}{4\pi} [K \cos(\theta) + i\lambda \cos(\theta + \phi)]\right\}, \quad (3)$$

whose norm takes the form

$$\mathcal{N}(t) = \int_{-\pi}^{\pi} |\psi(\theta, t)|^2 d\theta = I_0\left(\frac{\lambda t}{2\pi}\right). \quad (4)$$

Here, $I_0(x)$ denotes the modified Bessel function of the first kind with zeroth order [52]. The non-unitary evolution is characterized by the unbounded growth of the $\mathcal{N}(t)$ with time, i.e., $\mathcal{N}(t) \approx \exp(\lambda t/2\pi) \sqrt{2\pi/\lambda t}$ for $\lambda t/2\pi \gg 1$.

In the present work, we investigate both theoretically and numerically the dynamics of the momentum current $\langle p(t) \rangle$, energy diffusion $\langle p^2(t) \rangle$, and quantum scrambling $C(t) = -\langle [A(t), B]^2 \rangle$ [53–55]. Note that the $C(t)$ is defined in the Heisenberg picture, with $A(t) = U^\dagger(t) A U(t)$ and $\langle \cdot \rangle = \langle \psi(t_0) | \cdot | \psi(t_0) \rangle$ indicates the expectation value of the operator with respect to the initial state [56, 57]. To reduce the impact of the norm to observables, we introduce the rescaled quantities as $\langle p(t) \rangle = \sum_n p_n |\psi_n|^2 / \mathcal{N}(t)$ and $\langle p^2(t) \rangle = \sum_n p_n^2 |\psi_n|^2 / \mathcal{N}(t)$. We use the operators $A = e^{-i\varepsilon p}$ and $B = |\psi(t_0)\rangle\langle\psi(t_0)|$ to construct OTOCs. Straightforward derivation yields the relation $C(t) = \mathcal{N}^2(t) - |\langle \psi(t) | e^{-i\varepsilon p} | \psi(t) \rangle|^2$. Then, a natural definition of the rescaled OTOCs is given by $C(t) = 1 - |\langle \psi(t) | e^{-i\varepsilon p} | \psi(t) \rangle|^2 / \mathcal{N}^2(t)$ [58]. We consider the case $\varepsilon \ll 1$. Our main results are described by the three following relations

$$\langle p(t) \rangle = -K \sin(\phi) \frac{I_1\left(\frac{\lambda t}{2\pi}\right)}{I_0\left(\frac{\lambda t}{2\pi}\right)} t, \quad (5)$$

$$\langle p^2(t) \rangle = K^2 \sin^2(\phi) t^2 + \frac{2\pi}{\lambda} \frac{I_1\left(\frac{\lambda t}{2\pi}\right)}{I_0\left(\frac{\lambda t}{2\pi}\right)} [K^2 \cos(2\phi) + \lambda^2] t, \quad (6)$$

and

$$C(t) \approx K^2 \varepsilon^2 \sin^2(\phi) t^2 \left\{ 1 - \left[\frac{I_1\left(\frac{\lambda t}{2\pi}\right)}{I_0\left(\frac{\lambda t}{2\pi}\right)} \right]^2 \right\} + \frac{2\pi \varepsilon^2 t}{\lambda} \frac{I_1\left(\frac{\lambda t}{2\pi}\right)}{I_0\left(\frac{\lambda t}{2\pi}\right)} [K^2 \cos(2\phi) + \lambda^2], \quad (7)$$

where $I_1(x)$ denotes the modified Bessel function of the first kind with order one [52].

A. Directed current

Figure 1(a) shows that, for a specific λ (e.g., $\lambda = 0.3$), the $\langle p \rangle$ increases in the quadratic function of time for short time evolutions, and eventually transitions to linear growth. Such a transition occurs around a critical time t_c . In addition, one can see perfect agreement between numerical results and theoretical prediction in Eq. (5). For $\lambda t/2\pi \ll 1$, we have the approximations $I_0(\lambda t/2\pi) \approx 1$ and $I_1(\lambda t/2\pi) \approx \lambda t/4\pi$ [52]. Taking these relations to Eq. (5) yields the relation $\langle p(t) \rangle \approx -K \lambda \sin(\phi) t^2/4\pi$. Apparently, the growth rate $\langle p(t) \rangle/t^2 = -K \lambda \sin(\phi)/4\pi$ increases with the increase of λ , which is validated by our numerical results. For $\lambda t/2\pi \gg 1$, substituting the approximations of both $I_0(\lambda t/2\pi) \approx \exp(\lambda t/2\pi) (1 + \pi/4\lambda t) / \sqrt{\lambda t}$

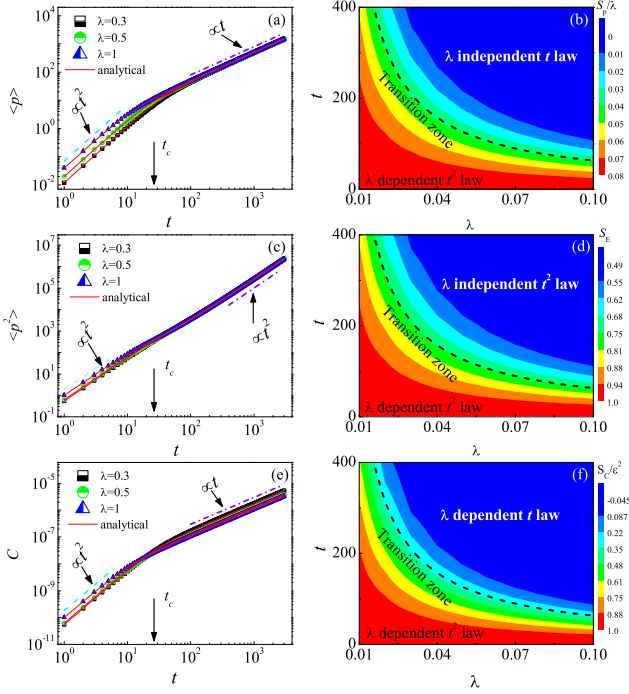


FIG. 1: Left panels: Time dependence of the $\langle p \rangle$ (a), $\langle p^2 \rangle$ (c), and C (e) for $\lambda = 0.3$ (squares), 0.5 (circles), and 1 (triangles). Red solid lines in (a), (c), and (e) indicate our theoretical predictions in Eqs. (5), (6), and (7), respectively. Arrows mark the threshold value of t_c . Green-dashed lines denote a square function of time. Violet dash-dotted lines in (a) and (e) denote the linear function of time, while in (b) it indicates the square function of time. Right panels: The values of S_p/λ (b), S_E (d), and S_C/ε^2 (f) in the parameter space (t, λ), which show three distinct zones. Dashed lines denote $t_c = 2\pi/\lambda$. In (e) and (f), the translation parameter is $\varepsilon = 10^{-5}$. The parameters are $K = 1$ and $\phi = -\pi/6$.

and $I_1(\lambda t/2\pi) \approx \exp(\lambda t/2\pi)(1 - 3\pi/4\lambda t)/\sqrt{\lambda t}$ [52] into Eq. (5) results in the linear growth $\langle p(t) \rangle \approx -K \sin(\phi)(t - \pi/|\lambda|)$, which is independent on λ when $t \gg 1$. The above estimations uncover the mechanism for the transition from quadratic-law growth to the linear growth as time evolves. In addition, our findings of the sinusoidal relationship between mean momentum and phase ϕ pave the way for Floquet engineering of the directed current in non-Hermitian chaotic systems.

To reveal whether there is singularity for the transition of the $\langle p \rangle$ from the short time to long time behavior, we investigate the second derivative of the mean momentum $S_p = d^2\langle p(t) \rangle/dt^2$. Note that, in the following derivation, for brevity, we use I_j to replace $I_j(\frac{\lambda t}{2\pi})$

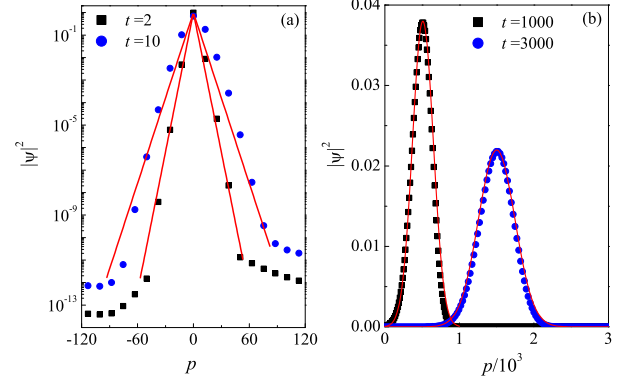


FIG. 2: Momentum distributions for short (a) and long (b) time evolution with $\lambda = 0.3$. In (a), red solid lines indicate the exponential fitting $|\psi(p)|^2 \sim \exp(-|p|/\xi)$ with $\xi = 2.1$ and 3.43 for $t = 2$ and 10 respectively. In (b), red solid lines indicate the Gaussian function fitting $|\psi(p)|^2 \sim \exp[-(p-p_c)^2/\sigma]$ with $(p_c = 500, \sigma = 3.9 \times 10^4)$ and $(p_c = 1500, \sigma = 1.2 \times 10^5)$ for $t = 1000$ and 3000 respectively. Other parameters are same as in Fig. 1(a).

($j = 0, 1, 2, \dots$). The analytical expression takes the form

$$S_p = -K \sin(\phi) \frac{\lambda}{2\pi} \left[1 + \frac{I_2}{I_0} - 2 \left(\frac{I_1}{I_0} \right)^2 \right] + K \sin(\phi) \frac{\lambda^2 t}{4\pi^2} \left[\frac{3I_1 - I_3}{4I_0} + \frac{3I_1 I_2}{2I_0^2} - 2 \left(\frac{I_1}{I_0} \right)^3 \right]. \quad (8)$$

Taking into account the approximation of I_j ($j = 0, 1, 2, 3$) under two different conditions, namely, when $\lambda t/2\pi \ll 1$ and when $\lambda t/2\pi \gg 1$ [52], we can derive approximate expressions

$$S_p \approx \begin{cases} \frac{-K \sin(\phi)\lambda}{2\pi}, & \text{for } \frac{\lambda t}{2\pi} \ll 1, \\ 0, & \text{for } \frac{\lambda t}{2\pi} \gg 1, \end{cases} \quad (9)$$

In Fig. 1(b), we have plotted the ratio S_p/λ for various values of t and λ . Three distinct zones can be observed: i) a λ dependent t^2 -law zone with $S_p/\lambda = -K \sin(\phi)/2\pi$ for $t \ll t_c = 2\pi/\lambda$; ii) a λ independent t -law zone with $S_p = 0$ for $t \gg t_c$; and iii) a transition zone for $t \sim t_c$.

In the λ dependent t^2 -law zone, the quantum state is exponentially localized in momentum space, i.e., $|\psi(p)|^2 \sim \exp(-|p|/\xi)$, whose localization length ξ increases with time [see Fig. 2(a)]. Detailed observations reveal that this exponentially-localized shape of the quantum state is asymmetric around $p = 0$. This kind of asymmetric spreading of the quantum state in momentum space results in the growth of mean momentum with time. While in the λ independent t -law zone, the momentum distribution can be well described by the Gaussian function $|\psi(p)|^2 \sim \exp[-(p-p_c)^2/\sigma]$ [see Fig. 2(b)]. Interestingly, the comparison of the momentum distribution in different time demonstrates that the center momentum p_c linearly increases with time, i.e., $p_c(t) = Dt$

for which the growth rate equal to that of the $\langle p(t) \rangle$, i.e., $D = d\langle p(t) \rangle/dt$. Therefore, the linear growth of the mean momentum for $t \gg t_c$ originates from the directed movement of the soliton-like wavepacket in momentum space. In addition, we would like to stress that the width σ of the Gaussian wavepacket also increases with time.

B. Energy diffusion

Figure 1(c) illustrates that the NQKR exhibits ballistic energy diffusion over time, specifically, $\langle p^2(t) \rangle = Gt^2$, which is in perfect agreement with our theoretical prediction in Eq. (6). Interestingly, for $t \ll t_c$, the diffusion rate G increases with the non-Hermitian parameter λ , and for $t \gg t_c$, it becomes independent of λ . By approximating both $I_0(\lambda t/2\pi)$ and $I_1(\lambda t/2\pi)$ under two different limits, we can derive the approximate expression for Eq. (6), namely, $\langle p^2(t) \rangle \approx (K^2 + \lambda^2)t^2/2$ for $t \ll t_c$ and $\langle p^2(t) \rangle \approx K^2 \sin^2(\phi)t^2 + 2\pi t [K^2 \cos(2\phi) + \lambda^2]/|\lambda|$ for $t \gg t_c$. This confirms the transition from λ -dependent behavior to λ -independent behavior. This transition can also be observed in the second derivative of the mean square of momentum, denoted as $S_E = d^2\langle p^2(t) \rangle/dt^2$,

$$S_E = 2K^2 \sin^2(\phi) - \frac{2\pi S_p}{K\lambda \sin(\phi)} [K^2 \cos(2\phi) + \lambda^2], \quad (10)$$

which can be approximated as

$$S_E \approx \begin{cases} K^2 + \lambda^2, & \text{for } \frac{\lambda t}{2\pi} \ll 1, \\ 2K^2 \sin^2(\phi), & \text{for } \frac{\lambda t}{2\pi} \gg 1. \end{cases} \quad (11)$$

In Figure 1(d), we present numerical results of S_E based on Eq. (10), which demonstrates the λ -dependent zone for $t \ll t_c$, a transition zone for $t \sim t_c$, and the λ -independent zone for $t \gg t_c$. Our discovery of the sinusoidal dependence of S_E on phase ϕ provides a theoretical foundation for engineering the energy diffusion through non-Hermitian driven potential.

C. Quantum scrambling

Based on the Taylor expansion $e^{-i\varepsilon p} \approx 1 - i\varepsilon p$ for $\varepsilon \ll 1$, we obtain the relations

$$\begin{aligned} C(t) &\approx \varepsilon^2 [\langle p^2 \rangle - \langle p \rangle^2] \\ &= K^2 \varepsilon^2 \sin^2(\phi) t^2 \left[1 - \left(\frac{I_1}{I_0} \right)^2 \right] \\ &\quad + \frac{2\pi \varepsilon^2 t I_1}{\lambda I_0} [K^2 \cos(2\phi) + \lambda^2], \end{aligned} \quad (12)$$

which has two different asymptotic behaviors

$$C(t) \approx \begin{cases} \frac{\varepsilon^2 (K^2 + \lambda^2)}{2} t^2, & \text{for } \lambda t/2\pi \ll 1, \\ \frac{2\pi \varepsilon^2}{|\lambda|} \left[\frac{1 + \cos(2\phi)}{2} K^2 + \lambda^2 \right] t, & \text{for } \lambda t/2\pi \gg 1. \end{cases} \quad (13)$$

In Fig. 1(c), we show our numerical results for the time evolution of C for different λ . It is evident that C exhibits a quadratic growth with time for $t \ll t_c$ and a linear growth with time for $t \gg t_c$, with both behaviors being dependent on λ . These distinct behaviors are also characterized by the second derivative $S_C = d^2C(t)/dt^2$. Straightforward derivation yields the relation

$$S_C = \varepsilon^2 \left[S_E - 2 \left(\frac{d\langle p \rangle}{dt} \right)^2 - 2\langle p \rangle S_p \right], \quad (14)$$

with

$$\frac{d\langle p \rangle}{dt} = -K \sin(\phi) \left\{ \frac{\lambda t}{4\pi} \left[1 + \frac{I_2}{I_0} - 2 \left(\frac{I_1}{I_0} \right)^2 \right] + \frac{I_1}{I_0} \right\}. \quad (15)$$

By approximating the terms on the right side of Eq.(14) under two different limits, we derive the approximate relation

$$S_C \approx \begin{cases} \varepsilon^2 (K^2 + \lambda^2), & \text{for } \lambda t/2\pi \ll 1, \\ 0, & \text{for } \lambda t/2\pi \gg 1. \end{cases} \quad (16)$$

Our numerical results, based on Eq. (14), clearly demonstrate the λ -dependent quadratic growth zone for $t \ll t_c$, the transition zone for $t \sim t_c$, and the λ -dependent linear growth zone for $t \gg t_c$ [see Fig. 1(f)], validating our theoretical prediction in Eq.(16).

D. Some remarks on the relation between phase manipulation and \mathcal{PT} -symmetry

The dependence of the long-time behavior of the $\langle p \rangle$, $\langle p^2 \rangle$ and C on the phase ϕ opens the opportunity for the manipulation of both the quantum transport and quantum scrambling via the relative phase between the real part and the imaginary part of the kicking potential $V_K(\theta) = K \cos(\theta) + i\lambda \cos(\theta + \phi)$ [see Eq. (2)]. Interestingly, the potential is \mathcal{PT} -symmetric when $\phi = \pi/2$. In this situation, both directed current and energy diffusion reach their maximum values, namely, $\langle p \rangle \approx -Kt$

Phase ϕ	$\pi/2$	π
Symmetry class	\mathcal{PT}	non- \mathcal{PT}
Directed current $\langle p(t) \rangle \propto K \sin(\phi)t$	$\propto Kt$	0
Energy diffusion $\langle p^2(t) \rangle \propto K^2 \sin^2(\phi)t^2 + 2\pi [K^2 \cos(2\phi) + \lambda^2] t/ \lambda $	$\propto K^2 t^2$	$\propto \frac{2\pi}{ \lambda } (K^2 + \lambda^2) t$
Quantum scrambling $C(t) \propto$ $\frac{2\pi \varepsilon^2}{ \lambda } \left[\frac{1 + \cos(2\phi)}{2} K^2 + \lambda^2 \right] t$	$\propto 2\pi \varepsilon^2 \lambda t$	$\propto \frac{2\pi \varepsilon^2}{ \lambda } (K^2 + \lambda^2) t$

TABLE I: Symmetry and the long-time behavior of the $\langle p \rangle$, $\langle p^2 \rangle$, and C for $\phi = \pi/2$ and π .

and $\langle p^2 \rangle \approx K^2 t^2$ since $\langle p \rangle$ and $\langle p^2 \rangle$ are sinusoidal functions of ϕ , signaling the \mathcal{PT} -symmetry protected transport behaviors. In contrast, quantum scrambling is minimized, i.e., $C \approx 2\pi\varepsilon^2|\lambda|t$ because C behaves as a cosine function of 2ϕ (see Table. I). For $\phi = \pi$, the NQKR model is a general non-Hermitian system that does not have \mathcal{PT} -symmetry, for which the directed current is totally suppressed, namely, $\langle p \rangle = 0$, and the energy diffusion reduces as $\langle p^2 \rangle \propto t$. In contrast the C is maximum $C \approx 2\pi\varepsilon^2 t(K^2 + \lambda^2)/|\lambda|$ demonstrating the non-Hermiticity enhanced quantum scrambling.

III. CONCLUSION AND DISCUSSIONS

One effective strategy for modulating quantum dynamics involves implementing Floquet driven potentials in systems, which has been accomplished by state-of-the-art experiments in both atom optics and optical waveguides. In this work, we investigate the interesting problems of the phase modulation of the directed current, energy diffusion and quantum scrambling, in a NQKR model with quantum resonance condition. We uncover a dynamical crossover in time-dependent behaviors of these phenomena. For short time interval $t \ll t_c$, the $\langle p \rangle$, $\langle p^2 \rangle$, and C all exhibit quadratic growth with time, and their growth rates depend on λ . After sufficiently long time evolution $t \gg t_c$, the $\langle p \rangle$ shows a linear growth independent of λ , the $\langle p^2 \rangle$ transitions to the λ -independent quadratic growth with time, and the C exhibits a linear growth dependent on the λ . These exotic behaviors are in perfect agreement with our theoretically predictions. Based on the second derivative, namely, S_p , S_E and S_C of these observables, we obtain the phase diagram of the crossover in the parameter space (t, λ) , which clearly presents three distinct zones for the dynamics of the momentum current, quantum diffusion and quantum scrambling.

In the atom-optics experiment, the complex potential in Eq.(2) has been realized by the superposition of two standing laser fields, interacting with ultracold atoms that encompass a ground state E_1 , excited states with two hyperfine levels E_2^\pm , and a non-interacting state E_i [26, 27]. The far-tuned standing laser, coupling E_1 and

E_2^- , generates a dipole force on the atoms, emulating the real component of the complex potential. The resonance laser facilitates the transition from E_1 to E_2^+ . The ultracold atoms in E_2^+ subsequently transition to E_i , resulting in particle loss and thereby mimicking the imaginary part of the complex potential. The precise modulation of the relative phase between the real and imaginary parts of the complex potential is achievable by adjusting the distance between the atomic beam and the mirror surface. The delta-kicking potential is emulated using a sequence of short square pulses created through the modulation of the standing wave by an acousto-optical modulator [24]. Consequently, our system in Eq. (1) is achievable in the state-of-the-art atom-optics experiments. Both the expectation values, such as $\langle p \rangle$ and $\langle p^2 \rangle$, and the variance can be detected via time-of-flight measurement of the probability density in momentum space [16, 22], which paves the way for the experimental validation of our findings.

Acknowledgments

Wen-Lei Zhao is supported by the National Natural Science Foundation of China (Grant Nos. 12065009 and 12365002), the Natural Science Foundation of Jiangxi province (Grant Nos. 20224ACB201006 and 20224BAB201023) and the Science and Technology Planning Project of Ganzhou City (Grant No. 202101095077). Jie Liu is supported by the NSAF (Contract No. U2330401).

Appendix A: Properties of the modified Bessel functions of the first kind

The modified Bessel functions of the first kind are defined by

$$I_m(x) = \frac{1}{2\pi} \int_0^{2\pi} e^{-im\theta} \exp[x \cos(\theta)] d\theta. \quad (\text{A1})$$

The function $I_m(x)$ can be expanded as

$$I_m(x) = \frac{e^x}{\sqrt{2\pi x}} \left[1 - \frac{4m^2 - 1}{8x} + \frac{(4m^2 - 1)(4m^2 - 9)}{2!(8x)^2} - \frac{(4m^2 - 1)(4m^2 - 9)(4m^2 - 25)}{3!(8x)^3} + \dots \right]. \quad (\text{A2})$$

Our theoretical analysis involves the function $I_m(x)$ with $0 \leq m \leq 3$. For $x \ll 1$, they can be approximated as

$$I_0(x) \approx 1, I_1(x) \approx \frac{x}{2}, I_2(x) \approx \frac{x^2}{8}, \text{ and } I_3(x) \approx \frac{x^3}{48}. \quad (\text{A3})$$

For $x \gg 1$, the two leading terms in Eq. (A2) contribute significantly. Therefore, we have neglected the other terms and obtained the following relations

$$I_0(x) \approx \frac{e^x}{\sqrt{2\pi x}} \left(1 + \frac{1}{8x} \right), \quad (\text{A4})$$

$$I_1(x) \approx \frac{e^x}{\sqrt{2\pi x}} \left(1 - \frac{3}{8x}\right), \quad (\text{A5}) \quad \text{and}$$

$$I_2(x) \approx \frac{e^x}{\sqrt{2\pi x}} \left(1 - \frac{15}{8x}\right), \quad (\text{A6})$$

$$I_3(x) \approx \frac{e^x}{\sqrt{2\pi x}} \left(1 - \frac{35}{8x}\right). \quad (\text{A7})$$

-
- [1] A. Kenfack, J. B. Gong, and A. K. Pattanayak, Controlling the Ratchet Effect for Cold Atoms, *Phys. Rev. Lett.* **100**, 044104 (2008).
- [2] C. Hainaut, A. Rançon, J. Clément, J. C. Garreau, P. Szriftgiser, R. Chicireanu, and D. Delande, Ratchet effect in the quantum kicked rotor and its destruction by dynamical localization *Phys. Rev. A* **97**, 061601(R) (2018).
- [3] Z. Q. Li, X. X. Hu, J. P. Xiao, Y. J. Chen, and X. B. Luo, Ratchet current in a \mathcal{PT} -symmetric Floquet quantum system with symmetric sinusoidal driving, *Phys. Rev. A* **108**, 052211 (2023).
- [4] D. Poletti, G. Benenti, G. Casati, and B. W. Li, Interaction-induced quantum ratchet in a Bose-Einstein condensate, *Phys. Rev. A* **76**, 023421 (2007).
- [5] J. B. Gong and P. Brumer, Coherent Control of Quantum Chaotic Diffusion, *Phys. Rev. Lett.* **86**, 1741 (2001).
- [6] M. Bitter and V. Milner, Experimental Demonstration of Coherent Control in Quantum Chaotic Systems, *Phys. Rev. Lett.* **118**, 034101 (2017).
- [7] M. A. Sentef, J. J. Li, F. Künzel, and M. Eckstein, Quantum to classical crossover of Floquet engineering in correlated quantum systems, *Phys. Rev. Research* **2**, 033033 (2020).
- [8] S. Y. Bai and J. H. An, Floquet engineering to reactivate a dissipative quantum battery, *Phys. Rev. A* **102**, 060201(R) (2020).
- [9] C. A. Downing and M. S. Ukhary, A quantum battery with quadratic driving, *Commun. Phys.* **6**, 322 (2023).
- [10] E. J. Meier, J. Ang'ong'a, F. Alex An, and B. Gadway, Exploring quantum signatures of chaos on a Floquet synthetic lattice, *Phys. Rev. A* **100**, 013623 (2019).
- [11] J. H. Wang *et. al.*, Information scrambling dynamics in a fully controllable quantum simulator, *Phys. Rev. Research* **4**, 043141 (2022).
- [12] J. Harris, B. Yan, and N. A. Sinitsyn, Benchmarking Information Scrambling, *Phys. Rev. Lett.* **129**, 050602 (2022).
- [13] Q. Q. Cheng, Y. M. Pan, H. Q. Wang, C. S. Zhang, D. Yu, A. Gover, H. J. Zhang, T. Li, L. Zhou, and S. N. Zhu, Observation of Anomalous π Modes in Photonic Floquet Engineering, *Phys. Rev. Lett.* **122**, 173901 (2019).
- [14] X. G. Wang, L. L. Zeng, G. H. Guo, and J. Berakdar, Floquet Engineering the Exceptional Points in Parity-Time-Symmetric Magnonics, *Phys. Rev. Lett.* **131**, 186705 (2023).
- [15] J. B. Gong and P. Brumer, Phase Control of Nonadiabaticity-Induced Quantum Chaos in an Optical Lattice, *Phys. Rev. Lett.* **88**, 203001 (2002).
- [16] C. Hainaut, I. Manai, J.-F. Clément, J. C. Garreau, P. Szriftgiser, G. Lemarié, N. Cherroret, D. Delande, and R. Chicireanu, Controlling Symmetry and Localization with an Artificial Gauge Field in a Disordered Quantum System, *Nat. Commun.* **9**, 1382 (2018).
- [17] C. Tian and A. Altland, Theory of localization and resonance phenomena in the quantum kicked rotor, *New J. Phys.* **12**, 043043 (2010).
- [18] J. C. Garreau and V. Zehnlé, Analog quantum simulation of the spinor-four Dirac equation with an artificial gauge field, *Phys. Rev. A* **101**, 053608 (2020).
- [19] G. Casati, I. Guarneri and D. L. Shepelyansky, Anderson transition in a onedimensional system with three incommensurate frequencies. *Phys. Rev. Lett.* **62**, 345 (1989).
- [20] D. L. Shepelyansky, Localization of diffusive excitation in multi-level systems, *Phys. D* **28**, 103 (1987).
- [21] C. S. Tian, A. Altland, and M. Garst, Theory of the Anderson Transition in the Quasiperiodic Kicked Rotor, *Phys. Rev. Lett.* **107**, 074101 (2011).
- [22] C. Hainaut, P. Fang, A. Rançon, J. F. Clément, Pascal Szriftgiser, J. C Garreau, C. S. Tian, and R. Chicireanu, Experimental Observation of a Time-Driven Phase Transition in Quantum Chaos, *Phys. Rev. Lett.* **121**, 134101 (2018).
- [23] M. Lopez, J. F. Clément, P. Szriftgiser, J. C. Garreau, and D. Delande, Experimental Test of Universality of the Anderson Transition *Phys. Rev. Lett.* **108**, 095701 (2012).
- [24] M. Lopez, J. F. Clément, G. Lemarié, D. Delande, P. Szriftgiser and J. C. Garreau, Phase diagram of the anisotropic Anderson transition with the atomic kicked rotor: theory and experiment, *New J. Phys.* **15** 065013 (2013).
- [25] I. Manai, J. Clément, R. Chicireanu, C. Hainaut, J. C. Garreau, P. Szriftgiser, and D. Delande, Experimental Observation of Two-Dimensional Anderson Localization with the Atomic Kicked Rotor, *Phys. Rev. Lett.* **115**, 240603 (2015).
- [26] D. O. Chudesnikov and V. P. Yakovlev, Bragg scattering on complex potential and formation of super-narrow momentum distributions of atoms in light fields, *Laser Phys.* **1**, 110 (1991).
- [27] C. Keller, M. K. Oberthaler, R. Abfalterer, S. Bernet, J. Schmiedmayer, and A. Zeilinger, *Phys. Rev. Lett.* **79**, 3327 (1997).
- [28] C. M. Bender and S. Boettcher, Real Spectra in Non-Hermitian Hamiltonians Having PT Symmetry, *Phys. Rev. Lett.* **80**, 5243 (1998).
- [29] J. B. Gong and Q. H. Wang, Time-dependent \mathcal{PT} -symmetric quantum mechanics, *J. Phys. A* **46**, 485302 (2013).
- [30] C. Wang, W. R. Sweeney, A. D. Stone, and L. Yang, Coherent perfect absorption at an exceptional point, *Science* **373**, 1261 (2021).
- [31] Ş. K. Özdemir, S. Rotter, F. Nori, and L. Yang, Parity-time symmetry and exceptional points in photonics, *Nature materials* **18**, 783 (2019).
- [32] Y. Song, W. Liu, L. Zheng, Y. Zhang, B. Wang, and P. Lu, Two-dimensional non-hermitian skin effect in a synthetic photonic lattice, *Phys. Rev. Applied* **14**, 064076

- (2020).
- [33] H. C. Li, C. Luo, T. L. Zhang, X. Zhou, J. W. Xu, J. W. Xu, S. X. Duan, X. H. Deng, Y. Shen, Non-Hermitian total-loss high-order topological insulator based on 1D Su–Schrieffer–Heeger (SSH), *Physica B: Condensed Matter*.
- [34] Y. Shen, *et al.*, Realization of Photonic Topological Insulators at Terahertz Frequencies Characterized by Time-Domain Spectroscopy, *Phys. Rev. Applied* **18**, 064025 (2022).
- [35] H. C. Li, C. Luo, T. L. Zhang, J. W. Xu, X. Zhou, Y. Shen, and X. H. Deng, Topological Refraction in Kagome Split-Ring Photonic Insulators, *Nanomaterials* **12**, 1493 (2022).
- [36] L. Zhang, *et al.*, Acoustic non-hermitian skin effect from twisted winding topology, *Nat. Commun.* **12**, 6297 (2021).
- [37] X. F. Zhu, H. Ramezani, C. Z. Shi, J. Zhu, and X. Zhang, \mathcal{PT} -Symmetric Acoustics, *Phys. Rev. X* **4**, 031042 (2014).
- [38] H. X. Zhang, T. Chen, L. H. Li, C. H. Lee, and X. D. Zhang, Electrical circuit realization of topological switching for the non-Hermitian skin effect, *Phys. Rev. B* **107**, 085426 (2023).
- [39] M. Chitsazi, H. N. Li, F. M. Ellis, and T. Kottos, Experimental Realization of Floquet \mathcal{PT} -Symmetric Systems, *Phys. Rev. Lett.* **119**, 093901 (2017).
- [40] K. Sim, N. Defenu, P. Mognini, and R. Chitra, Quantum Metric Unveils Defect Freezing in Non-Hermitian Systems, *Phys. Rev. Lett.* **131**, 156501 (2023).
- [41] W. Y. Wang, B. Sun, and J. Liu, Adiabaticity in non-reciprocal Landau-Zener tunneling, *Phys. Rev. A* **106**, 063708 (2022).
- [42] X. Q. Tong, X. L. Gao, and S. P. Kou, Adiabatic-impulse approximation in the non-Hermitian Landau-Zener model, *Phys. Rev. B* **107**, 104306 (2023).
- [43] X. Wang, H. D. Liu, and L. B. Fu, Nonlinear non-Hermitian Landau-Zener–Stückelberg–Majorana interferometry, *New J. Phys.* **25** 043032 (2023).
- [44] W. L. Zhao, J. Z. Wang, X. H. Wang, and P. Q. Tong, Directed momentum current induced by the \mathcal{PT} -symmetric driving, *Phys. Rev. E* **99**, 042201 (2019).
- [45] W. L. Zhao, Quantization of out-of-time-ordered correlators in non-Hermitian chaotic systems, *Phys. Rev. Research* **4**, 023004 (2022).
- [46] W. L. Zhao, R. R. Wang, H. Ke, and J. Liu, Scaling laws of the out-of-time-order correlators at the transition to the spontaneous \mathcal{PT} -symmetry breaking in a Floquet system, *Phys. Rev. A* **107**, 062201 (2023).
- [47] K. Yokomizo and S. Murakami, Non-bloch band theory of nonhermitian systems, *Phys. Rev. Lett.* **123**, 066404 (2019).
- [48] F. Song, S. Yao, and Z. Wang, Non-hermitian skin effect and chiral damping in open quantum systems, *Phys. Rev. Lett.* **123**, 170401 (2019).
- [49] L. W. Zhou, D.-J. Zhang, Non-Hermitian Floquet Topological Matter—A Review, *Entropy* **25**, 1401 (2023).
- [50] H. Y. Meng, Y. S. Ang, and C. H. Lee, Exceptional points in non-Hermitian Photonics: Applications and Recent Developments, arXiv:2310.16699.
- [51] H. Cao and J. Wiersig, Dielectric microcavities: Model systems for wave chaos and non-hermitian physics, *Rev. Mod. Phys.* **87**, 61 (2015).
- [52] See Appendix for the properties of modified Bessel function $I_n(x)$.
- [53] Z. Qi, T. Scaffidi, and X. Cao, Surprises in the deep Hilbert space of all-to-all systems: From superexponential scrambling to slow entanglement growth, *Phys. Rev. B* **108**, 054301 (2023).
- [54] X. D. Hu, T. Luo, and D. B. Zhang, Quantum algorithm for evaluating operator size with Bell measurements, *Phys. Rev. A* **107**, 022407 (2023).
- [55] J. Wang, G. Benenti, G. Casati, and W. G. Wang, Quantum chaos and the correspondence principle, *Phys. Rev. E* **103**, L030201 (2021).
- [56] S. Pappalardi and Jorge Kurchan, Low temperature quantum bounds on simple models, *SciPost Phys.* **13**, 006 (2022).
- [57] R. J. Lewis-Swan, A. Safavi-Naini, J. J. Bollinger, and A. M. Rey, Unifying scrambling, thermalization and entanglement through measurement of fidelity out-of-time-order correlators in the Dicke model, *Nat. Commun.* **10**, 1581 (2019).
- [58] W. L. Zhao and J. Liu, Quantum criticality at the boundary of the non-Hermitian regime of a Floquet system, arXiv:2307.00462.